Journal of Geospatial Surveying (2022) 2:2
DOI: http://doi.org/10.4038/jgs.v2i2.37

ORIGINAL ARTICLE

A Preliminary Analysis Towards Detecting Floating Marine Macro Plastics Using an Index Developed for Sentinel 2 ACOLITE and Sen2Cor Images

Pathira Arachchilage, K. R. L.[a,b,c], Tang, D.[*a,b], Yu, J.[a,b], Wang, S.[a]

[a]*State Key Laboratory of Tropical Oceanography, Guangdong Key Laboratory of Ocean Remote Sensing, South China Sea Institute of Oceanology, Chinese Academy of Sciences; Southern Marine Science and Engineering Guangdong Laboratory (Guangzhou), Guangzhou 511458, China*

[b]*University of Chinese Academy of Sciences, Beijing 100049, China*

[c]*Sabaragamuwa University of Sri Lanka, P.O. Box 02, Belihuloya, 70140, Sri Lanka*

ARTICLE INFO

Article history:
Received 7 June 2022
Received in revised form 18 July 2022
Accepted 1 August 2022
Available online 19 August 2022

Keywords:
Marine harvested macro plastic
ACOLITE
Sen2Cor
Index
Scatter plots

ABSTRACT

The improper management of plastic waste has become a silent killer in the marine ecosystem. The scientific evidence of plastic accumulated in marine biota and entering the food web have urged quick actions against the plastic pollution. The plastic detection algorithms developed using satellite images can proclaim emission, transportation, weathering and accumulation of plastic that is vital in eliminating them. This study developed an index to find floating marine harvested macro plastic within Sentinel 2 ACOLITE and Sen2Cor images. This index preserved the plastic information protected the plastic information and maximized the separation of them from the surrounding objects. The identified plastic pixels were analysed using scatter plots to discriminate plastic from non-plastic objects and to observe the characteristics. The index and the scatter plot analysis detected the plastic pixels with bottle percentages more than or equal to 14%. The plastic bags and the fishing nets required around 50% pixel percentage to be detected. The plastic pixels with 100% plastic coverage were located as a separate cluster in the scatter plots. Therefore, the accurate detection of plastic pixels using ACOLITE and Sen2Cor images depends on the pixel plastic percentage and plastic coverage. The Sen2Cor images classified plastic pixels according to their pixel plastic percentage for two dates. However, this classification was not successful for other dates with aerosol, clouds and smooth sea surface conditions which made the plastic signal weak. The ACOLITE and Sen2Cor atmospheric corrections are not suitable for plastic detection when the plastic signal is weak.

1 Introduction

Marine plastic is an emerging threat and decisions should be taken deliberately before the worst-case scenarios happen. Plastics tend to be accumulated almost everywhere in the ocean, including sea surface, water column, seafloor, shoreline, and marine organisms (Brignac et al., 2019; IUCN, 2021). In addition, plastic pollution is detrimental to marine biota, and cause severe injuries and deaths by ingesting or entangling of plastic debris (Barboza et al., 2020; Gregory, 2009; Thiel et al., 2018; Thushari and Senevirathna, 2020). Recent efforts of scientists have discovered the plastic in remote coral reefs and atolls. Diverse micro plastic polymers which exhibited the characteristics of long distance transportation were found near these reefs and atolls (Yu et al., 2022). Furthermore, recent studies suggest that the climate change and the marine plastic pollution are linked together. Greenhouse gas emission is considered as one of the primary causes of this link (Ford et al., 2022). Understanding the plastic cycle between emission and accumulation is vital to detect marine plastic.

Many studies have been conducted on marine plastic pollution addressing emission (Lebreton et al., 2017; Meijer et al., 2021), transportation (Declerck et al., 2019; NOAA, 2016), and accumulation (Eriksen et al., 2014; Lacerda et al., 2019). Furthermore, there are a number of attempts to

* Corresponding author: D. Tang, State Key Laboratory of Tropical Oceanography, Guangdong Key Laboratory of Ocean Remote Sensing, South China Sea Institute of Oceanology, Chinese Academy of Sciences; Southern Marine Science and Engineering Guangdong Laboratory (Guangzhou), Guangzhou 511458, China.

E-mail address: lingzistdl@126.com (D. Tang).

[*] The previous version of the same article has been replaced with this version where **Fig. 1** has been corrected.

remotely detect these plastic (Davaasuren et al., 2018; Kikaki et al., 2020; Kremezi et al., 2021; Mifdal et al., 2021; Park et al., 2021; Tasseron et al., 2021). The remote detection of plastic in the marine environment using satellites is still in its developing stage. This study focused on remote detection of floating marine macro plastic using Sentinel 2 ACOLITE and Sen2Cor data.

Scientists have already examined the possibilities of utilizing Sentinel 2 for macro plastic detection with different methods (Biermann et al., 2020; Themistocleous et al., 2020; Topouzelis et al., 2020; Topouzelis et al., 2019). The plastic was identified using Sentinel 2 ACOLITE and Sen2Cor corrected images from the plastic litter project (PLP) 2018 (Topouzelis et al., 2019). In addition, PLP 2019 Sentinel 2 data were analysed for plastic using match filtering technique. This algorithm recognized plastic pixels with a minimum abundance fraction of 25% (Topouzelis et al., 2020). However, even though there were plastic detection techniques invented using Sentinel 2 ACOLITE and Sen2Cor images in the previous studies, still there were uncertainties cause by glint, clouds and aerosols in accurate identification of plastic. The Sentinel 2 data processed with several indices like floating debris index (FDI), normalized difference vegetation index (NDVI), and plastic index (PI) were the recent attempts of identifying plastic (Biermann et al., 2020; Themistocleous et al., 2020). Moshtaghi et al.(2021) found that the plastic detection method using FDI and NDVI proposed by Biermann et al. (2020) is depending highly on the type of plastic and the concentration of suspended sediments.

This study investigated a method to extend the plastic detection while minimizing uncertainties caused by the methods used in previous studies. The aims of this study were; (1) building an index to detect marine debris including plastic in the satellite images (2) detecting plastic pixels with less than 25% of plastic pixel coverage, and (3) discriminating plastic from other non-plastic objects.

2 Methodology

2.1 Study Sites

The Sentinel 2 images were collected for Mytilene (Greece) (Topouzelis et al., 2020; Topouzelis et al., 2019) and Cyprus (Themistocleous et al., 2020). These study sites had ocean harvested plastic data. The plastic patches were harvested in the Tasmakia beach, Greece, under the PLP 2018 and 2019 projects. The dates of these data were 07/06/2018 (AA), 18/04/2019 (BB), 03/05/2019 (CC), 18/05/2019 (DD), 28/05/2019 (EE) and 07/06/2019 (FF). Here the notations of AA, BB, CC, DD, EE and FF are given for the dates of Mytilene data.

The Fig. 1 indicates the names and the locations of the plastic pixels in Mytilene identified in this study. The ocean harvested plastic data for Cyprus was extracted on 15/12/2018.

2.2 Sentinel 2 Data Preparation

The ACOLITE allows coastal and inland water processing for applications like sediment flows, oil spills, and chlorophyll levels. It contains two atmospheric correction methodologies using exponential extrapolation function and dark spectrum fitting (RBINS, 2020). The dark spectrum fitting was used as the correction methodology in this study. The ACOLITE version used was OLI lite Version 20190326.0. The Sentinel 2 level 1C images were converted into level 2A images using the Sen2Cor v2.9 plugin. The default configuration of Sen2Cor v2.9 is similar to the L2A core product in Sentinel 2 satellite ground segment. Therefore, no further adjustment is required for acquiring L2A core products. In addition, this plugin is helpful in level 2A products generation for historical Sentinel 2A images (ESA, 2020).

The ACOLITE and Sen2Cor atmospheric corrections were used in this study as they were proven to be effective in detecting floating marine macro plastics. The ACOLITE corrected FDI and NDVI images classified mixed materials and identified plastics with 86% of accuracy. The ACOLITE corrected images, after processing with match filtering technique, identified plastic pixels with pixel percentage as low as 25% (Biermann et al., 2020; Topouzelis et al., 2020; Topouzelis et al., 2019). Therefore, the initial steps of plastic monitoring were taken with the images corrected with ACOLITE and Sen2Cor. This study further used them for testing the new index. All of these images were resampled into 10 m resolution before further processing. In addition, a land mask was applied to all images using a threshold applied to 1610 nm band. The 1610 nm band was selected to identify the land areas because the reflectance values between land and water varied significantly in a way that water contained lower values and land areas contained higher values.

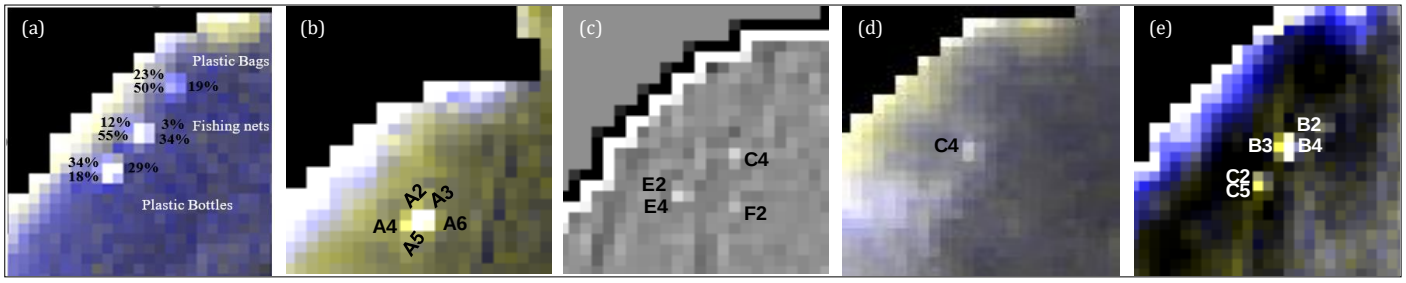

Fig. 1: The Mytilene plastic pixels' names and their locations for different dates of (a) AA (b) BB (c) CC (d) DD (e) FF

2.3 Defining an Algorithm for Floating Plastic

Researchers have been investigating algorithms to detect plastic using Sentinel 2 imagery. Recently, FDI combined with NDVI was used to identify plastic from other materials like sea water, sea weed, timber, sea foam and pumice (Biermann et al., 2020). Furthermore, normalized difference water index (NDWI), water ratio index (WRI), automated water extraction index (AWEI), modified normalization difference water index (MNDWI), normalization difference moisture index (NDMI), simple ratio (SR), PI, and reversed normalized difference vegetation index (RNDVI) were used to find the ocean harvested plastic in Cyprus (Themistocleous et al., 2020). Here we developed an index to find the debris pixels including plastic, while minimizing the limitations and uncertainties introduced in the above indexes.

This index was developed using Sentinel 2 near-infrared (NIR), red, and short wave infrared (SWIR) bands as in Eq. 1. It was calculated as the difference between NIR reflectance and its baseline reflectance ($R'_{Rf,NIR}$).The baseline reflectance was calculated as a linear interpolation between red and SWIR bands. The subtracted baseline of the index is expected to remove possible atmospheric disturbances. The maximum chlorophyll index (MCI), floating algae index (FAI), and FDI were also calculated by subtracting a baseline reflectance from the band which contained a relatively higher reflectance for the examined object (Alikas et al., 2010; Biermann et al., 2020; Hu, 2009). The baselines serve as atmospheric correction algorithms and sensitivity minimizing algorithms for surrounding objects. The formatting in this index is quite similar to FAI (Hu, 2009). FAI used the difference between 859 nm and a baseline between 645 nm and 1240 nm that is more sensitive to floating algae. In this study, we used the difference between Sentinel 2 NIR, and its baseline reflectance to maximize the plastic response in the image.

$$Index = R_{Rf,NIR} - R'_{Rf,NIR}$$

$$R'_{Rf,NIR} = \frac{\lambda_{NIR} - \lambda_{RED}}{\lambda_{SWIR} - \lambda_{RED}} \left(R_{Rf,SWIR} - R_{Rf,RED}\right) - R_{Rf,RED}$$

$$Index = R_{Rf,NIR} + R_{Rf,RED} - \frac{\lambda_{NIR} - \lambda_{RED}}{\lambda_{SWIR} - \lambda_{RED}} \left(R_{Rf,SWIR} - R_{Rf,RED}\right) \quad (1)$$

In this index, the R_{Rf} refers to the reflectance. The SWIR band (1613.7 nm/1610.4 nm) was used to correct the atmospheric errors. The strong absorption of light in NIR, and SWIR wavelength regions by relatively low turbid water surfaces was analysed by many water-related research (Martins et al., 2017; Pereira-Sandoval et al., 2019; Ruddick et al., 2000; Shi and Wang, 2009). The SWIR was further recommended to atmospherically correct high turbid coastal water areas (Pereira-Sandoval et al., 2019; Shi and Wang, 2009). Because of this capability of addressing different turbidity levels, SWIR wavelength was considered as the most convenient to correct atmospheric effects in this study. In addition, it is observed that floating plastic has a higher reflectance in the Sentinel 2 NIR (832.8 nm/833 nm) wavelength (Themistocleous et al., 2020; Topouzelis et al., 2019). The addition operation between NIR and red bands (664.6 nm/665 nm) could be converted to subtraction, such as in FAI, to remove majority of atmospheric disturbances in the image. However, it also removed the plastic information. Thus, the addition of red band reflectance to NIR reflectance served as a means to preserve plastic information. Therefore, this index as a whole protected the plastic information and maximized the separation of plastic pixels from the surrounding objects.

As the next step, the scatter plots between index applied images and Sentinel 2 bands of band 5 (704.1 nm/ 703.8 nm), band 8 (832.8 nm/833 nm) and band 9 (945.1 nm/ 943.2 nm) were analysed to separate plastic pixels from other substances. The 'X' axis values, 'Y' axis values and the clustering of the debris pixels were also observed using these scatter plots. The reflectance of materials like wood, timber, white caps, sea foam and rock in band 5 is higher than most of the plastic types, and it was observed in recent research work done by scientists (Biermann et al., 2020; Moshtaghi et al., 2021). Therefore, this band was selected especially with the purpose of discriminating plastic from these materials which are abundant in the marine environment. In addition, the studies have revealed that there is an absorption feature of plastic around ~931 nm (Garaba and Dierssen, 2018; Moshtaghi et al., 2021) and for ocean harvested plastic, this is observed as ~960 nm (Garaba et al., 2021). The band 9, which has a wavelength around these absorption features, was selected in order to aid the identification of plastic. Moreover, most of the materials like sea foam, Sargassum and timber contains a higher reflectance in band 8 similar to plastic (Biermann et al., 2020). Thus, this band was selected with the purpose of comparative analysis of all materials. ACOLITE corrected images were analysed by using two scatter plots due to the unavailability of band 9.

2.4 Evaluating the Derived Index with FDI and PI

The FDI and PI are the two indexes developed to detect floating marine debris and marine plastic respectively. The results of the index developed in this study were tested with the results given by these indexes to observe the efficiency of using the derived index.

3 Results

3.1 Index Applied ACOLITE and Sen2Cor images

Fig. 2 illustrates the results of index applied ACOLITE and Sen2Cor images of the study sites. The pixel names of PLP data used in this analysis are as Fig. 1 and pixel percentages/composition of different plastic materials for PLP 2018 and 2019 were referred from the original sources of Topouzelis et al. (2019) and Topouzelis et al. (2020).

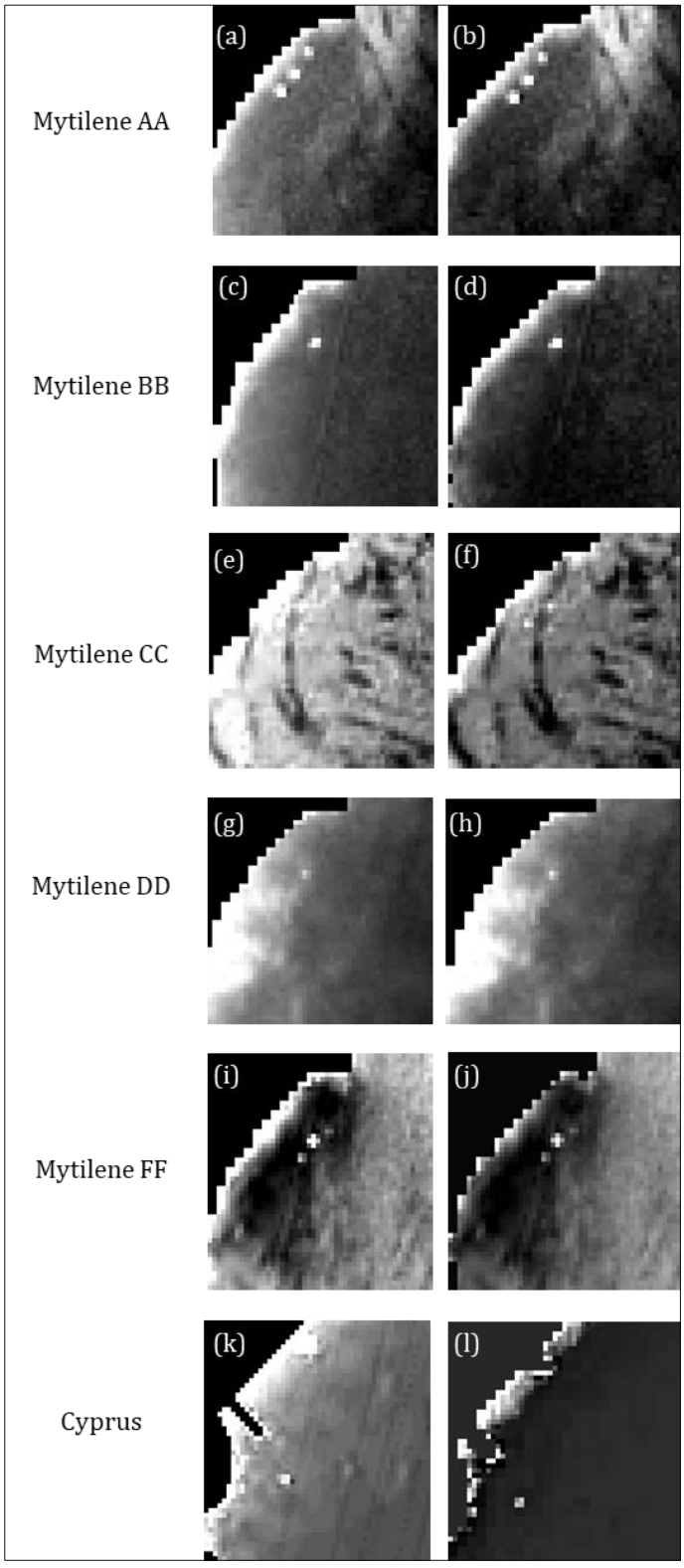

Fig. 2: ACOLITE index applied (left) and Sen2Cor index applied(right) images that indicate the detected ocean harvested plastic patches of Mytilene for the dates of AA, BB, CC, DD, FF and Cyprus

3.1.1 Plastic Pixel Identification of AA Index Applied ACOLITE and Sen2Cor Images

The Fig. 2(a) indicated pixels of plastic bottles 34%, 29%, 18%, fishing nets 55%, 12% and plastic bags 50% with higher reflectance values between 0.06 and 0.11. These pixels also had a good contrast with the background water pixels. The Fig. 2(b) delivered a similar result to Fig. 2(a).

3.1.2 Plastic Pixel Identification of BB Index Applied ACOLITE and Sen2Cor Images

Pixels of A2 (plastic bags 2%, plastic bottles 28%), A3 (plastic bags 0%, plastic bottles 18%), and A5 (plastic bags 18%, plastic bottles 15%) had reflectance values between 0.08 and 0.099 in Fig. 2(c). In addition, all plastic pixels, including A4 (plastic bags 38%, plastic bottles 0%) and A6 (plastic bags 0%, plastic bottles 1%), had a noticeable disparity between background water pixels. The Fig. 2(d) had reflectance values between 0.05 and 0.075 for A2, A3 and A5 pixels. In contrast, the A4, A6 pixel reflectance was lower.

3.1.3 Plastic Pixel Identification of CC Index Applied ACOLITE and Sen2Cor Images

The C4 (plastic bags 0%, plastic bottles 14%), F2 (plastic bags 0%, plastic bottles 21%), E2 (plastic bags 0%, plastic bottles 27%) and E4 (no plastic) were indicated in Fig. 2(f). However, the contrast between plastic pixels and water pixels was considerably decreased compared to the other dates. It was very difficult to differentiate C4, F2, E4 and E2 plastic pixels in Fig. 2(e) due to the conversion of the sea in to a rapidly changing heterogeneous background.

3.1.4 Plastic Pixel Identification of DD Index Applied ACOLITE and Sen2Cor Images

The Fig. 2(g) accentuated C4 pixel (plastic bottles 40%, plastic bags 0%). However, identifying this pixel was challenging due to the atmospheric disturbance (clouds or aerosols) nearby. The Fig. 2(h) showed similar results as Fig. 2(g).

3.1.5 Plastic Pixel Identification of EE Index Applied ACOLITE and Sen2Cor Images

It was not possible to identify the plastic pixels on EE image due to high sun glint present in the image.

3.1.6 Plastic Pixel Identification of FF Index Applied ACOLITE and Sen2Cor Images

The plastic pixels of C2 (plastic bags 1%, plastic bottles 54%), C5 (plastic bags 11%, plastic bottles 4%), and three reed pixels of B2, B3, and B4 with 18%, 20% and 4% of reeds respectively were featured in the Fig. 2(i). The reeds pixels were indicated with a higher contrast compared to the plastic pixels. The Fig. 2(j) showed an equivalent result to the Fig. 2(i).

3.1.7 Plastic Pixel Identification of Cyprus Index Applied ACOLITE and Sen2Cor Images

Four plastic pixels were detected in Fig. 2(k) and (l) similar to the results indicated by WRI, NDVI, NDMI and RNDVI of Themistocleous et al. (2020). The results cannot be discussed further as we do not have the data related to pixel-wise plastic percentage.

3.2 Scatter Plot Analysis

Fig. 3 indicates the scatter plot analysis of ACOLITE index applied images. The green colour is used to highlight the areas above the selected reference line.

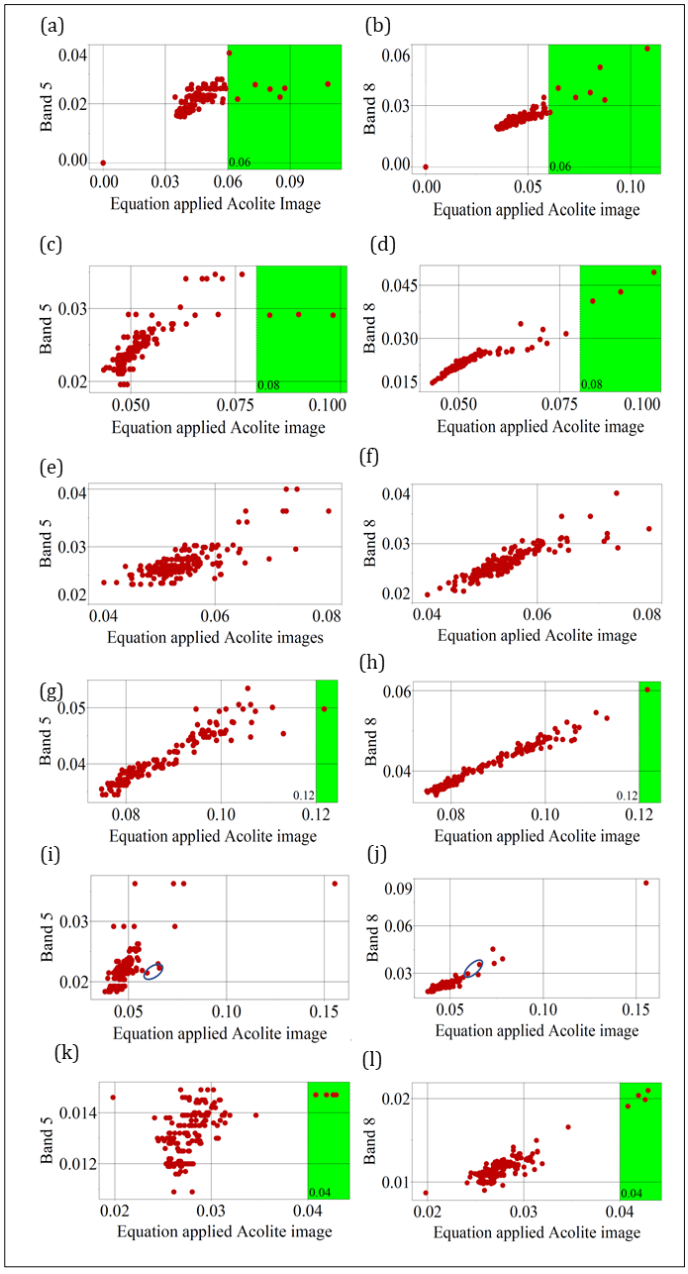

Fig. 3: ACOLITE Scatter plot analysis of (a-b) AA (c-d) BB (e-f) CC (g-h) DD (i-j) FF (k-l) Cyprus

Fig. 4 indicates the scatter plot analysis of Sen2Cor index applied images. The green colour is used to highlight the areas above the selected reference line.

3.2.1 AA

The plastic pixels of plastic bottles 34%, 29%, 18%, fishing nets 12%, 55% and plastic bags 50% were detected by analysing the scatter plots of Fig. 3(a), (b) and Fig. 4(a). The Fig. 4(b) delivered a similar result to the Fig. 3(b). The Fig. 4(c) indicated different clusters of plastic pixels such as plastic bottles 34%, 29%, 18% and fishing nets 55% (red ellipse) as a one category, fishing nets 12%(blue circle) and plastic bags 50% (black circle) pixels as two other separate categories.

3.2.2 BB

The Fig. 3(c) and (d) differentiated A2, A3, A5 pixels from background water pixels. The Fig. 4(d), (e), (f) indicated A2, A3, A5, A4, and A6 pixels as a separate cluster from water pixels. In addition, they detached these five pixels into two groups of A2, A3, A5 (black ellipse) and A4, A6 (blue ellipse). This differentiation was well established in the Fig. 4(e) and (f). The Fig. 4(d), (e), (f) A2, A3 and A5 pixels with high pixel plastic percentage could be observed with a 'X' axis value of 0.05 similar to Fig. 4(a), (b) and (c).

3.2.3 CC

The Fig. 3(e) and (f) did not successfully detect the plastic pixels. The E4 and C4 pixels were indicated as a separate cluster in the three scatter plots of Fig. 4(g), (h) and (i). The E2 pixel (black circle) is shown close to E4 and C4 only in the Fig. 4(h). However, this pixel was not detectable from the background water pixels using the reference line created to identify E4 and C4 at 0.048. The F2 pixel was not attained by Fig. 4(g), (h) and (i).

3.2.4 DD

The Fig. 3(g), (h) showed the C4 plastic pixel as a separate entity from the water cluster. This difference was conspicuous in the Fig. 3(h) due to the compact form of the water pixels. The C4 pixel could be extracted in the Fig. 4(j), (k) and (l) as it held the maximum 'X' value. However, the nearby pixels could easily cause uncertainty in the extraction.

3.2.5 EE

It was not possible to discriminate plastic pixels using scatter plot analysis of EE. The pixels did not show clusters, and instead they all were randomly spread.

3.2.6 FF

The plastic pixels could be identified in the Fig. 3(i) and (j) within close proximity to water and reed pixels (blue ellipse). Therefore, it was not easy to separate plastic and water. The same problem existed in the Sen2Cor image scatter plots.

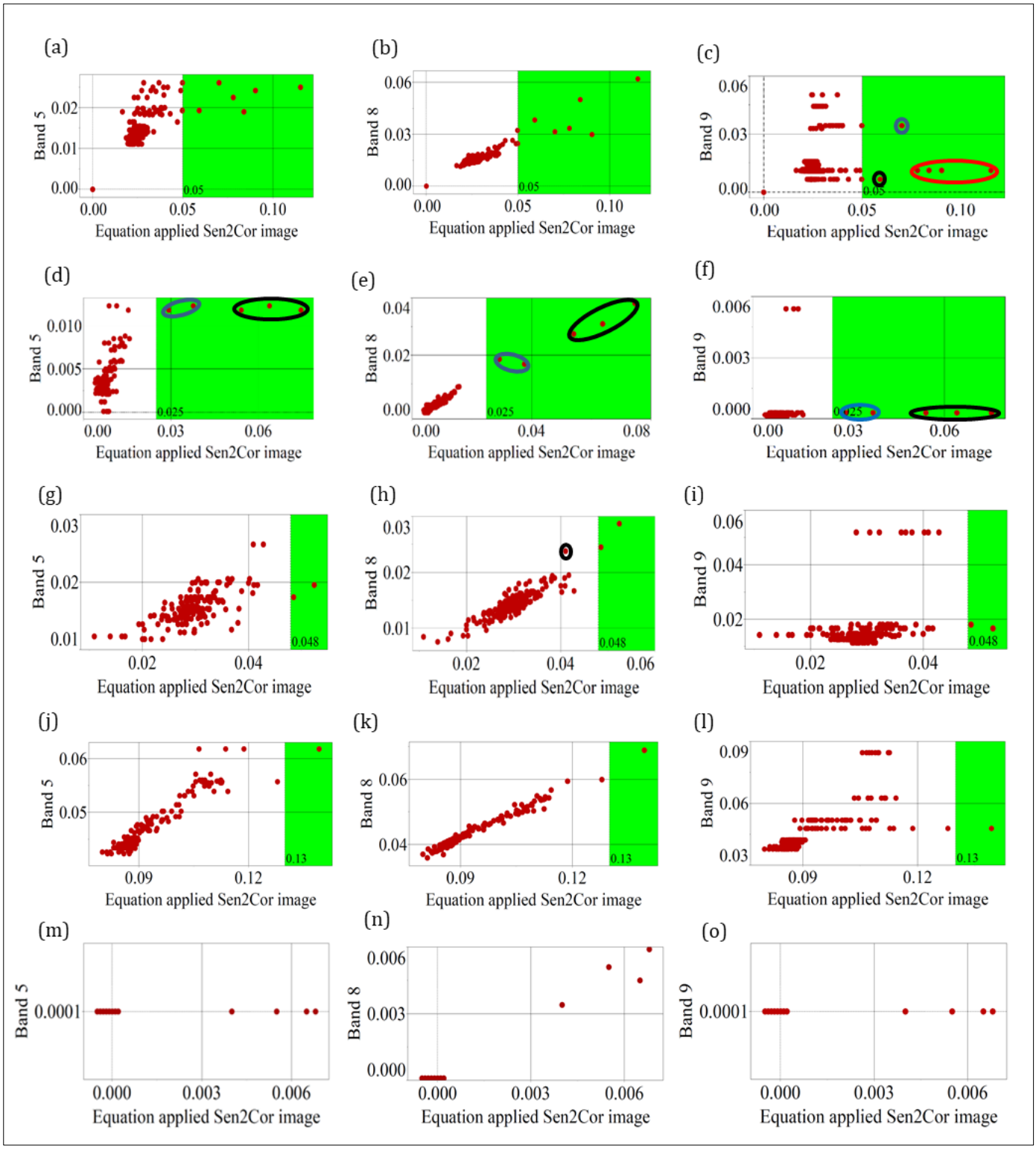

Fig. 4: Sen2Cor Scatter plot analysis of (a-c) AA (d-f) BB (g-i) CC (j-l) DD (m-o) Cyprus

3.2.7 Cyprus

The ACOLITE (Fig. 3(k), (l)) and Sen2Cor index applied images (Fig. 4(m), (n), (o)) detected the four plastic pixels. However, both ACOLITE and Sen2Cor bands, and index applied images produced low values for plastic compared to the other dates. Most notably, Sen2Cor band 5 and band 9 images produced the least value of all which was 0.0001.

The index applied Sen2Cor images indicated two special situations on AA and BB. For example, Fig. 4(c) derived three categories of plastic pixels with pixel close to shore pixels, another pixel closer to water pixels, and another separate set of pixels with high percentage plastic bottles (34%, 29% and 18%) and fishing nets pixels (55%). The

pixel at the close range to the shore pixels was composed of low plastic percentage fishing nets pixels (12%), proving the dominance of bottom reflectance on fishing nets plastic patch as mentioned in Topouzelis et al. (2019). In addition, plastic bag pixel (50%) observed nearby the water cluster explained that the difference between the optical characteristics of water and plastic bags is negligible, and therefore, the percentage of plastic bottles in a pixel significantly contributed to the capability of plastic detection. All plastic bottle pixels detected in this study proved this fact further. The Fig. 3(c-d) and Fig. 4(d-f) identified A2, A3, and A5 pixels. The Fig. 4(d-f) divided all the plastic pixels into two clusters of plastic bottles percentage more than or equal to 15 and less than or equal to 1. Even though these results are convincing, they were not uniform for all the dates. The extraction of plastic pixels from CC, DD, EE and FF ACOLITE and Sen2Cor index applied images were more complicated and irreconcilable due to smooth sea surface condition, aerosol/clouds, high glint and inseparability between different substances (water and reeds) respectively. The plastic pixels on FF were located very close to the water pixels. The pixel plastic coverage can be a possible reason for this proximity. Because all the other identified pixels by ACOLITE or Sen2Cor images had 100% plastic coverage. However, on FF, the plastic coverage was 25% (Topouzelis et al., 2020). The Sen2Cor scatter plot analysis of CC was not able to detect the F2 and E2 pixels. This complication of the CC image could be due to its sea surface state and illumination. The sea appeared relatively smooth on CC image which highlighted the small variations between neighbouring pixels by any stretching. The AA and BB Sen2Cor image pixels with high plastic percentage could be identified with a common reference value of 0.05. However, this could not be done on CC, DD, EE and FF due to the environmental perturbations and low plastic coverage. The weak plastic signals on these days were reduced further by ACOLITE and Sen2Cor index applied images and caused substantial uncertainties in plastic detection. The Sen2Cor images performed well in identifying plastic pixels for BB and CC than ACOLITE images.

4 Discussion

4.1 Building the Index

Indices like MCI, FAI, FDI and PI were studied thoroughly in deriving the index in this study (Alikas et al., 2010; Biermann et al., 2020; Hu, 2009; Themistocleous et al., 2020). The MCI and FAI are used to detect floating algae. In contrast, the FDI and PI are used to discover marine plastic. All the study sites in this study were examined using FDI and PI to check whether they work for plastic detection. The Fig. 5 below shows the FDI and PI image results for Mytilene on AA.

The application of FDI and PI on ACOLITE and Sen2Cor images did not identify all the plastic pixels similar to the index introduced in this study. The Fig. 5(a) indicates some of the plastic bottles, fishing nets and bags pixels. However, these pixels are difficult to identify with the rapidly changing heterogeneous water background and they are not contrasted from the water background similar to Fig. 2(a). The Fig. 5(b) also shows some plastic bottle pixels. However, many near shore pixels can cause uncertainty in identifying these plastic bottle pixels. Furthermore, the fishing nets and plastic bottle pixels are not indicated with a good contrast from the water background similar to Fig. 2(b). The plastic pixels are not identifiable in Fig. 5(c-d). The FDI or PI did not identify all the plastic pixels in these study sites, therefore this study investigated for a new index.

Previous research have revealed the importance of using a combination of visible, NIR and SWIR bands in detecting marine plastic litter to avoid any misinterpretations cause by the colour of plastic, shape of plastic, form of plastic and the presence of other materials like seaweed, oil slicks, sun glint, sea foam, white caps and bubbles (Garaba et al., 2021; Moshtaghi et al., 2021). The Index in this study considers the high reflectance of NIR (832.8 nm/833 nm) for plastic objects (Themistocleous et al., 2020; Topouzelis et al., 2019) and sensitivity of SWIR (1613.7 nm/1610.4 nm) band for atmospheric disturbances (Martins et al., 2017; Pereira-Sandoval et al., 2019; Ruddick et al., 2000; Shi and Wang, 2009). The red band (664.6 nm/665 nm) contains a considerable reflectance for plastic even though there is no reflectance peak such as for the NIR band. Therefore, the addition of red and NIR bands enhances the plastic information in the image.

The introduced index found all the plastic pixels in ACOLITE and Sen2Cor (Fig. 2) in a comprehensive manner. It disclosed most of the plastic pixels deployed off Mytilene and Cyprus which contained plastic bottle percentages more than or equal 14%. This percentage below 25% is very important as it has surpassed a limitation of plastic pixel detection in Sentinel 2 images using spectra analysis (Topouzelis et al., 2020). The plastic bags and fishing nets pixels require pixel percentages of 50% and 55% respectively to be detected. However, further research should be done to confirm these percentages for fishing nets as it is tested one time in AA image. The difficulty of detecting plastic bag pixels which was studied by Topouzelis et al. (2020) is emphasized again in this analysis.

4.2 Scatter Plot Analysis

The discrimination of plastic and non-plastic pixels was expected to be done using the scatter plot analysis. However, it was not successful using the ACOLITE and Sen2Cor images. The disadvantage of using ACOLITE and Sen2Cor atmospheric corrections in plastic detection is that they further weaken the plastic signals that are influenced by different sea surface conditions, glint and clouds/aerosols. Also, the accurate detection of plastic pixels using ACOLITE and Sen2Cor images depends on the pixel plastic percentage and plastic coverage. The scatter plots cluster the plastic pixels and water pixels separately when the plastic coverage is 100%.

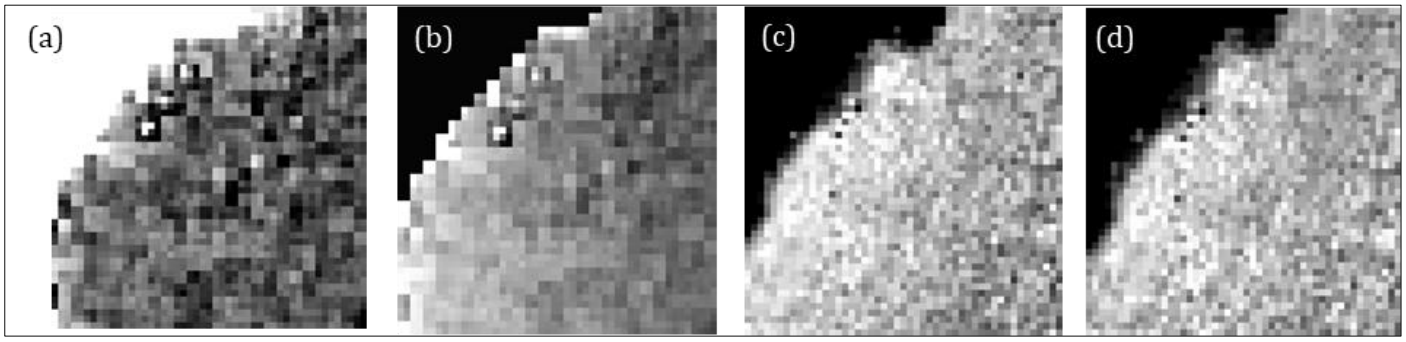

Fig. 5: Mytilene processed images of AA (a) ACOLITE FDI image (b) Sen2Cor FDI image (c) ACOLITE PI image (d) Sen2Cor PI image

When comparing ACOLITE and Sen2Cor scatter plot results, the Sen2Cor scatter plots perform well in identifying and clustering the plastic pixels on all the dates.

The scatter plots analysis was used by Biermann et al. (2020) for the automated classification of floating debris. The variables they used were FDI and NDVI and these indexes were calculated using the ACOLITE images. They identified different clusters for different types of marine debris using FDI and NDVI values. However, Moshtaghi et al. (2021) found that the method proposed by Biermann et al. (2020) is highly dependent on the type of plastic and the concentration of suspended sediments. Themistocleous et al. (2020) observed that the Sen2Cor atmospheric correction reduced the plastic reflectance for Cyprus. These studies indicate the dependence of ACOLITE and Sen2Cor single band values and index applied images on different external factors, and this study emphasized this further.

5 Conclusion

The index invented in this study discovered the marine harvested plastic using Sentinel 2 ACOLITE and Sen2Cor images. Both index and the scatter plot analysis detected plastic pixels with plastic bottle percentages more than or equal to 14%. The fishing nets and plastic bags required around 50% pixel percentage to be detected. The plastic pixels with 100% plastic coverage were located as a separate cluster from the water pixels in the scatter plot analysis. Therefore, factors like percentage of plastic within the pixel and total plastic coverage are influential factors for the accurate estimation of plastic pixels. Furthermore, ACOLITE and Sen2Cor atmospheric corrections are not suitable to detect plastic pixels when there are low plastic coverage and atmospheric disturbances such as aerosol, clouds and glint in the image. Because low plastic coverage and atmospheric disturbances make the plastic signal weak, and this weak signal is weakened further after applying ACOLITE or Sen2Cor.

Acknowledgement

This work was supported by Guangdong Special Support Program for Key Talents Team under grant [2019BT02H594]; Key Special Projects of Southern Marine Science and Engineering Guangdong Laboratory (Guangzhou) (for Introduced Talents Team) under grants [GML2021GD0810 , GML2019ZD0602], the National Natural Science Foundation of China under grants[41876136 and 41430968]; Guangdong Key Lab of Remote Sensing (LORS) under grant [2017B030301005]; Key Project of Guangdong Institute for International Strategic under grant [17ZDA24] and Innovation Academy of South China Sea Ecology and Environmental Engineering, Chinese Academy of Sciences under grant [ISEE2019ZR02].

Author Contributions

K.R.L.P.A contributed to the conceptualization, methodology, investigation, writing - original draft preparation, and visualization. T.D. contributed to the resources, funding acquisition, project administration, conceptualization, supervision, writing review and editing. W.S. contributed to investigation. Y.J. contributed to the formal analysis. All authors contributed to the article and approved the submitted version of the manuscript.

Conflict of Interest

The authors declare no conflict of interest.

References

Alikas, K., Kangro, K., Reinart, A., 2010. Detecting cyanobacterial blooms in large North European lakes using the Maximum Chlorophyll Index. Oceanologia. 52, 237-257. https://doi.org/10.5697/oc.52-2.237.

Barboza, L. G. A., Lopes, C., Oliveira, P., Bessa, F., Otero, V., Henriques, B., Raimundo, J., Caetano, M., Vale, C., Guilhermino, L., 2020. Microplastics in wild fish from North East Atlantic Ocean and its potential for causing neurotoxic effects, lipid oxidative damage, and human health risks associated with ingestion exposure. Science of the Total Environment. 717, 134625. https://doi.org/10.1016/j.scitotenv.2019.134625.

Biermann, L., Clewley, D., Martinez-Vicente, V., Topouzelis, K., 2020. Finding plastic patches in coastal waters

using optical satellite data. Scientific reports. 10, 1-10. https://doi.org/10.1038/s41598-020-62298-z.

Brignac, K. C., Jung, M. R., King, C., Royer, S.-J., Blickley, L., Lamson, M. R., Potemra, J. T., Lynch, J. M., 2019. Marine debris polymers on main Hawaiian Island beaches, sea surface, and seafloor. Environmental science & technology. 53, 12218-12226. https://doi.org/10.1021/acs.est.9b03561.

Davaasuren, N., Marino, A., Boardman, C., Alparone, M., Nunziata, F., Ackermann, N., Hajnsek, I., 2018. Detecting microplastics pollution in world oceans using SAR remote sensing. IGARSS 2018-2018 IEEE International Geoscience and Remote Sensing Symposium. IEEE, pp. 938-941.

Declerck, A., Delpey, M., Rubio, A., Ferrer, L., Basurko, O., Mader, J., Louzao, M., 2019. Transport of floating marine litter in the coastal area of the south-eastern Bay of Biscay: A Lagrangian approach using modelling and observations. Journal of Operational Oceanography. 12, S111-S125. https://doi.org/10.1080/1755876X.2019.1611708.

Eriksen, M., Lebreton, L. C., Carson, H. S., Thiel, M., Moore, C. J., Borerro, J. C., Galgani, F., Ryan, P. G., Reisser, J., 2014. Plastic pollution in the world's oceans: more than 5 trillion plastic pieces weighing over 250,000 tons afloat at sea. PloS one. 9, e111913. https://doi.org/10.1371/journal.pone.0111913.

ESA, 2020. European Space Agency. Sen2Cor v2.9. Sen2Cor – STEP, 1. Available from: http://step.esa.int/main/snap-supported-plugins/sen2cor/sen2cor-v2-9/. Accessed on 15.08.2020.

Ford, H. V., Jones, N. H., Davies, A. J., Godley, B. J., Jambeck, J. R., Napper, I. E., Suckling, C. C., Williams, G. J., Woodall, L. C., Koldewey, H. J., 2022. The fundamental links between climate change and marine plastic pollution. Science of The Total Environment. 806, 150392. https://doi.org/10.1016/j.scitotenv.2021.150392.

Garaba, S. P., Arias, M., Corradi, P., Harmel, T., de Vries, R., Lebreton, L., 2021. Concentration, anisotropic and apparent colour effects on optical reflectance properties of virgin and ocean-harvested plastics. Journal of Hazardous Materials. 406, 124290. https://doi.org/10.1016/j.jhazmat.2020.124290.

Garaba, S. P., Dierssen, H. M., 2018. An airborne remote sensing case study of synthetic hydrocarbon detection using short wave infrared absorption features identified from marine-harvested macro- and microplastics. Remote Sensing of Environment. 205, 224-235. https://doi.org/10.1016/j.rse.2017.11.023.

Gregory, M. R., 2009. Environmental implications of plastic debris in marine settings—entanglement, ingestion, smothering, hangers-on, hitch-hiking and alien invasions. Philosophical Transactions of the Royal Society B: Biological Sciences. 364, 2013-2025. https://doi.org/10.1098/rstb.2008.0265.

Hu, C., 2009. A novel ocean color index to detect floating algae in the global oceans. Remote Sensing of Environment. 113, 2118-2129. https://doi.org/10.1016/j.rse.2009.05.012.

IUCN, 2021. International Union for Conservation of Nature. Marine plastic pollution | IUCN. ISSUES Br., (November): 1. https://www.iucn.org/resources/issues-briefs/marine-plastic-pollution. Accessed on 19.12.2021.

Kikaki, A., Karantzalos, K., Power, C. A., Raitsos, D. E., 2020. Remotely sensing the source and transport of marine plastic debris in Bay Islands of Honduras (Caribbean Sea). Remote Sensing. 12, 1727. https://doi.org/10.3390/rs12111727.

Kremezi, M., Kristollari, V., Karathanassi, V., Topouzelis, K., Kolokoussis, P., Taggio, N., Aiello, A., Ceriola, G., Barbone, E., Corradi, P., 2021. Pansharpening PRISMA data for marine plastic litter detection using plastic indexes. IEEE Access. 9, 61955-61971. https://doi.org/10.1109/ACCESS.2021.3073903.

Lacerda, A. L. d. F., Rodrigues, L. d. S., Van Sebille, E., Rodrigues, F. L., Ribeiro, L., Secchi, E. R., Kessler, F., Proietti, M. C., 2019. Plastics in sea surface waters around the Antarctic Peninsula. Scientific reports. 9, 1-12. https://doi.org/10.1038/s41598-019-40311-4.

Lebreton, L., Van Der Zwet, J., Damsteeg, J.-W., Slat, B., Andrady, A., Reisser, J., 2017. River plastic emissions to the world's oceans. Nature Communications. 8, 1-10. https://doi.org/10.1038/ncomms15611.

Martins, V. S., Barbosa, C. C. F., De Carvalho, L. A. S., Jorge, D. S. F., Lobo, F. d. L., Novo, E. M. L. d. M., 2017. Assessment of atmospheric correction methods for Sentinel-2 MSI images applied to Amazon floodplain lakes. Remote Sensing. 9, 322. https://doi.org/10.3390/rs9040322.

Meijer, L. J., van Emmerik, T., van der Ent, R., Schmidt, C., Lebreton, L., 2021. More than 1000 rivers account for 80% of global riverine plastic emissions into the ocean. Science Advances. 7, eaaz5803. https://doi.org/10.1126/sciadv.aaz5803.

Mifdal, J., Longépé, N., Rußwurm, M., 2021. Towards detecting floating objects on a global scale with learned spatial features using sentinel 2.

Moshtaghi, M., Knaeps, E., Sterckx, S., Garaba, S., Meire, D., 2021. Spectral reflectance of marine macroplastics in the VNIR and SWIR measured in a controlled environment. Scientific Reports. 11, 1-12. https://doi.org/10.1038/s41598-021-84867-6.

NOAA, 2016. National Oceanic and Atmospheric Administration. Report on Modeling Oceanic Transport of Floating Marine Debris. Model. Ocean. Transp. Float. Mar. Debris, 21p. Available from: https://marinedebris.noaa.gov/reports/modeling-oceanic-transport-floating-marine-debris. Accessed on 05.12.2020.

Park, Y.-J., Garaba, S. P., Sainte-Rose, B., 2021. Detecting the Great Pacific Garbage Patch floating plastic litter using WorldView-3 satellite imagery. Optics Express. 29, 35288-35298. https://doi.org/10.1364/OE.440380.

Pereira-Sandoval, M., Ruescas, A., Urrego, P., Ruiz-Verdú, A., Delegido, J., Tenjo, C., Soria-Perpinyà, X., Vicente, E., Soria, J., Moreno, J., 2019. Evaluation of atmospheric correction algorithms over Spanish inland waters for sentinel-2 multi spectral imagery data. Remote Sensing. 11, 1469. https://doi.org/10.3390/rs11121469.

RBINS, 2020. Royal Belgian Institute of Natural Sciences. ACOLITE. Acolite - OD Nat., 1. Available from: https://odnature.naturalsciences.be/remsem/software-and-data/acolite. Accessed on 20.05.2020.

Ruddick, K. G., Ovidio, F., Rijkeboer, M., 2000. Atmospheric correction of SeaWiFS imagery for turbid coastal and inland waters. Applied optics. 39, 897-912. https://doi.org/10.1364/AO.39.000897.

Shi, W., Wang, M., 2009. An assessment of the black ocean pixel assumption for MODIS SWIR bands. Remote Sensing of Environment. 113, 1587-1597. https://doi.org/10.1016/j.rse.2009.03.011.

Tasseron, P., Van Emmerik, T., Peller, J., Schreyers, L., Biermann, L., 2021. Advancing floating macroplastic detection from space using experimental hyperspectral imagery. Remote Sensing. 13, 2335. https://doi.org/10.3390/rs13122335.

Themistocleous, K., Papoutsa, C., Michaelides, S., Hadjimitsis, D., 2020. Investigating detection of floating plastic litter from space using sentinel-2 imagery. Remote Sensing. 12, 2648. https://doi.org/10.3390/rs12162648.

Thiel, M., Luna-Jorquera, G., Álvarez-Varas, R., Gallardo, C., Hinojosa, I. A., Luna, N., Miranda-Urbina, D., Morales, N., Ory, N., Pacheco, A. S., 2018. Impacts of marine plastic pollution from continental coasts to subtropical gyres—fish, seabirds, and other vertebrates in the SE Pacific. Frontiers in Marine Science. 238. https://doi.org/10.3389/fmars.2018.00238.

Thushari, G. G. N., Senevirathna, J. D. M., 2020. Plastic pollution in the marine environment. Heliyon. 6, e04709. https://doi.org/10.1016/j.heliyon.2020.e04709.

Topouzelis, K., Papageorgiou, D., Karagaitanakis, A., Papakonstantinou, A., Arias Ballesteros, M., 2020. Remote sensing of sea surface artificial floating plastic targets with Sentinel-2 and unmanned aerial systems (plastic litter project 2019). Remote Sensing. 12, 2013. https://doi.org/10.3390/rs12122013.

Topouzelis, K., Papakonstantinou, A., Garaba, S. P., 2019. Detection of floating plastics from satellite and unmanned aerial systems (Plastic Litter Project 2018). International Journal of Applied Earth Observation and Geoinformation. 79, 175-183. https://doi.org/10.1016/j.jag.2019.03.011.

Yu, J., Wang, S., Tang, D., He, L., Lakshani, P. A. K. R., 2022. Spatial distribution and composition of surface microplastics in the southwestern South China Sea. Frontiers in Marine Science. 9: 830318. https://doi.org/10.3389/fmars.2022.830318.